PB89-197743

Onset of Electrical Breakdown in Dust Layers
1. Microsparking Described by Paschen's Law

(U.S.) Environmental Protection Agency
Research Triangle Park, NC

1988

U.S. Department of Commerce
National Technical Information Service
NTIS

TECHNICAL REPORT DATA
(Please read Instructions on the reverse before completing)

1. REPORT NO. EPA/600/J-88/253	2.	3. RI PB89-197743
4. TITLE AND SUBTITLE The Onset of Electrical Breakdown in Dust Layers: I. Microsparking Described by Paschen's Law		5. REPORT DATE 1988 6. PERFORMING ORGANIZATION CODE
7. AUTHOR(S) Ronald P. Young and James L. DuBard (SoRI); and Leslie E. Sparks (AEERL)		8. PERFORMING ORGANIZATION REPORT NO.
9. PERFORMING ORGANIZATION NAME AND ADDRESS Southern Research Institute P.O. Box 55305 Birmingham, Alabama 35255-5305		10. PROGRAM ELEMENT NO. 11. CONTRACT/GRANT NO. CR808973 and CR810284
12. SPONSORING AGENCY NAME AND ADDRESS EPA, Office of Research and Development Air and Energy Engineering Research Laboratory Research Triangle Park, NC 27711		13. TYPE OF REPORT AND PERIOD COVERED Journal Article; 5-11/87 14. SPONSORING AGENCY CODE EPA/600/13

15. SUPPLEMENTARY NOTES AEERL's author/project officer is Leslie E. Sparks, Mail Drop 54, 919/541-2458. Published in JAPCA, 38:11, pp. 1412-1418, 11/88.

16. ABSTRACT The paper describes a study of the onset of electrical breakdown in dust layers, for hand-deposited dust layers in a parralel-plate geometry. It was found that the breakdown was an ordinary electron avalanche process originating in voids within the dust layer and obeying Paschen's Law. The size of voids where breakdown occurs was in the range of 10-20 micrometers for the layers used. The distribution of particle sizes in a sample influences its breakdown through changes in the average void dimension where breakdown takes place. Water vapor in the test environment, which affects the electrical conduction mechanism prior to breakdown, lowered the average electric field required to initiate breakdown. Moderate compaction of the sample had little or no effect on its breakdown behavior.

17. KEY WORDS AND DOCUMENT ANALYSIS

a. DESCRIPTORS	b. IDENTIFIERS/OPEN ENDED TERMS	c. COSATI Field/Group
Pollution Dust Electrostatic Precipitators Electrical Faults Avalanche Breakdown Particle Size Distribution Electric Corona	Pollution Control Stationary Sources Paschen's Law Microsparking	13B 11G 14G 13I 20C

18. DISTRIBUTION STATEMENT Release to Public	19. SECURITY CLASS (This Report) Unclassified	21. NO. OF PAGES 10
	20. SECURITY CLASS (This page) Unclassified	22. PRICE MF $0.95/PC $4.95

EPA Form 2220-1 (9-73)

REPRODUCED BY
U.S. DEPARTMENT OF COMMERCE
NATIONAL TECHNICAL INFORMATION SERVICE
SPRINGFIELD, VA. 22161

EPA/600/J-88/253

JAPCA 38: 1412-1418 (1988)

The Onset of Electrical Breakdown in Dust Layers: I. Microsparking Described by Paschen's Law

Ronald P. Young and James L. DuBard
Southern Research Institute
Birmingham, Alabama

Leslie E. Sparks
U.S. Environmental Protection Agency
Research Triangle Park, North Carolina

The onset of electrical breakdown in dust layers has been studied for hand-deposited dust layers in a parallel plate geometry. It was found that the breakdown was an ordinary electron avalanche process originating in voids within the dust layer and obeying Paschen's Law. The size of voids where breakdown occurs was in the range of 10 to 20 μm for the layers used. The distribution of particle sizes in a sample influences its breakdown through changes in the average void dimension where breakdown takes place. Water vapor in the test environment, which affects the electrical conduction mechanism prior to breakdown, lowered the average electric field required to initiate breakdown. Moderate compaction of the sample had little or no effect on its breakdown behavior.

The negative corona current in an electrostatic precipitator induces a large voltage drop across the dust layer on the collecting electrode which can become large enough to initiate electrical breakdown within the dust layer. Sustained breakdown within the dust layer leads to a back discharge of positive ions into the precipitator gas stream, resulting in deterioration of precipitator performance. This study was motivated by a need to understand the factors contributing to the onset of electrical breakdown in dust layers in an electrostatic precipitator.

In this study, a dust layer was hand-deposited between parallel plate electrodes, and the applied potential was slowly increased until the first microspark in the dust layer was observed on an oscilloscope. The parallel plate geometry provided a well-defined, uniform average electric field across the dust layer and allowed standard resistivity measurements to be performed. The non-destructive nature of the breakdown measurement allowed systematic tests to be performed on a single sample. Mercury porosimetry analysis on each sample was used to correlate the breakdown behavior with the distribution of voids within the samples.

It was found that the onset of electrical breakdown in the dust samples could be explained as ordinary electron avalanche breakdown across gas-filled voids in the dust layer, the dimension of such voids being on the order of a few tens of micrometers. This process was affected by the particle size distribution through changes in the dimension of voids where breakdown occurred. Moderate mechanical compaction of the dust layer had little or no effect on its breakdown behavior. The presence of water vapor in the test environment, which affects the electrical conduction mechanism prior to breakdown, generally lowered the average electric field across the dust layer necessary to initiate breakdown.

Materials and Methods

The components of the apparatus used in these experiments are shown schematically in Figure 1. The dust layer was hand-deposited between the parallel plates of the test cell to a uniform depth of 0.5 cm using a constant surface areal loading of 10 g/cm^2. Negative polarity high voltage was applied to the top electrode and the guarded center electrode was connected, by means of a switch (SW), to either an electrometer (A) for resistivity measurements or an oscilloscope (OSC) for electrical breakdown measurements. The loaded test cell was placed into an environmental chamber and maintained at 250°C overnight in dry air. The following morning, humid air was introduced and the system was allowed to equilibrate for at least 1 hour before beginning measurements.

Dust Samples

Three dust species were chosen for this investigation: two pulverized coal fly ashes (Sundance and Wabamun) and a Portland cement dust (Lehigh). The chemical analyses of

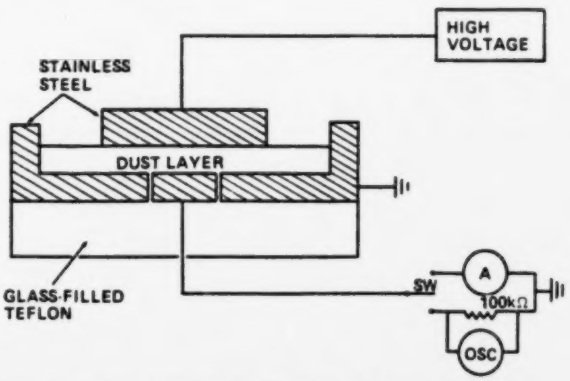

Figure 1. Schematic diagram for electrical breakdown measurements.

these three dusts are shown in Table I. The label "ordinary" refers to the as-received samples; "fine" and "coarse" refer to size-fractionated samples. The two fly ashes are virtually identical in nature except for their Na content, with Sundance having 5 to 6 times the amount of Na as Wabamun fly ash. Since Na is believed to be the dominant conductor of ionic charge in fly ash,[1,2] data for these two species were

Copyright 1988—APCA

NTIS is authorized to reproduce and sell this report. Permission for further reproduction must be obtained from the copyright owner.

Table I. Chemical analysis of dust samples by weight percent.

	Sundance fly ash			Wabamun fly ash			Lehigh cement dust		
	Ordinary MMD = 12.3 μm	Fine (MMD < 5 μm)	Coarse (MMD > 50 μm)	Ordinary MMD = 33.5 μm	Fine (MMD < 5 μm)	Coarse (MMD > 50 μm)	Ordinary MMD = 15.2 μm	Fine (MMD < 5 μm)	Coarse (MMD > 50 μm)
Li_2O	0.01	0.01	0.01	0.01	0.01	0.01	<0.01	<0.01	<0.01
Na_2O	1.9	2.4	1.0	0.34	0.49	0.34	0.03	0.03	0.05
K_2O	0.51	0.57	0.48	0.73	1.1	0.58	0.33	0.51	0.24
MgO	1.3	1.4	0.99	1.8	1.9	1.5	1.3	0.92	0.99
CaO	10.4	11.7	10.5	10.5	9.6	11.0	43.5	45.7	43.1
Fe_2O_3	3.6	3.8	3.8	3.4	3.3	3.9	1.6	1.4	2.0
Al_2O_3	22.5	23.1	21.7	21.2	21.5	19.3	3.6	5.0	0.98
SiO_2	54.8	52.0	60.0	58.4	57.8	60.8	12.6	8.5	20.2
TiO_2	0.92	0.83	0.83	1.1	0.83	0.83	0.2	0.2	0.33
P_2O_5	0.18	0.19	0.14	0.17	0.16	0.10	0.06	0.06	0.04
SO_3	0.34	0.50	0.13	0.33	0.61	0.14	0.29	0.35	0.29
LOI[a]	0.58	0.39	2.0	0.53	0.66	1.2	35.7	37.1	33.5

[a] Loss on ignition at 750°C.

expected to provide information on the role of charge carrier concentration in the breakdown process. The fly ash particles are predominantly spherical in shape and amorphous; while cement dust is a more crystalline material with irregularly shaped particles and is chemically quite different from fly ash.

Resistivity Measurements

The resistivity measurement was made according to the general procedures listed in the IEEE Standard 548-1984, descending temperature method only. While increasing the field across the sample from zero to 4 kV/cm required for the measurement, the oscilloscope was monitored to be sure breakdown did not occur. After the current was measured for the resistivity determination, the voltage was immediately removed from the dust layer. In no case did breakdown occur before achieving a field of 4 kV/cm. Moreover, resistivity measurements made with this apparatus and those made with a standard resistivity test cell under equivalent conditions were in good agreement.

Breakdown Measurements

The breakdown measurement was performed by slowly increasing the voltage across the dust layer while observing the oscilloscope until the breakdown signal[3] appeared as a single pulse. Since the peak amplitudes of the breakdown signals were usually in the range of 25 to 50 mV, the oscilloscope was operated at a sensitivity of 20 mV/div. A sweep rate of 20 μs/div (corresponding to 200 μs for a single sweep) was used to observe the complete breakdown signal. The voltage reading on the power supply meter (the average breakdown voltage, V_{BD}, across the dust layer) was recorded and the applied voltage was immediately removed from the sample. The temperature of the environmental chamber was then stabilized at a lower temperature and these measurements were repeated. In this manner, data were obtained at approximately 15 degree increments from 250°C down to 100°C. The data obtained were found to be reproducible for different samples of a given dust species under identical conditions. In addition, resistivity measurements of a virgin dust sample were the same as those obtained after performing breakdown measurements on the sample.

Results

The parameters which were studied for their effect on the onset of electrical breakdown in dust layers fall into two categories: environmental factors (sample temperature and atmospheric moisture) and dust species (chemical composition, particle shape, and void size distribution). For the majority of the tests, the three dust species behaved qualitatively the same. Therefore, the results presented here will focus on the Wabamun fly ash, with any species-dependent characteristics pointed out when appropriate.

Environmental Effect on Breakdown

The variation of average breakdown voltage, V_{BD} (or average electric field at breakdown, E_{BD}) with temperature and atmospheric humidity for Wabamun fly ash is shown in Figure 2. V_{BD} is the power supply reading (negative polarity) at the occurrence of the first microspark on the oscilloscope. E_{BD} is obtained by dividing V_{BD} by the layer thickness, 0.5 cm. The indicated water levels in the atmosphere are in volume percent. Because we were interested in preserving the sample for further tests, no systematic measurements of breakdown were made at electric fields higher than those which produced the first microspark. However, we noted

Table II. Porosimetry and density of samples.

Sample distribution		Largest void radius detected by mercury porosimetry (μm)	Mean void radius (μ_{L3})	Density (g/cc)	Porosity (%)
Wabamun	Ordinary	53.13	8.44	2.19	49.4
	Fine	40.39	8.88	2.33	66.0
	Coarse	53.94	11.77	2.08	40.7
Sundance	Ordinary	51.05	8.07	2.08	53.7
	Fine	52.39	8.94	2.21	65.6
	Coarse	51.92	9.58	1.99	47.0
Lehigh	Ordinary	35.29	7.70	2.67	60.3
	Fine	27.87	8.13	2.66	70.3
	Coarse	44.82	12.16	2.69	41.6

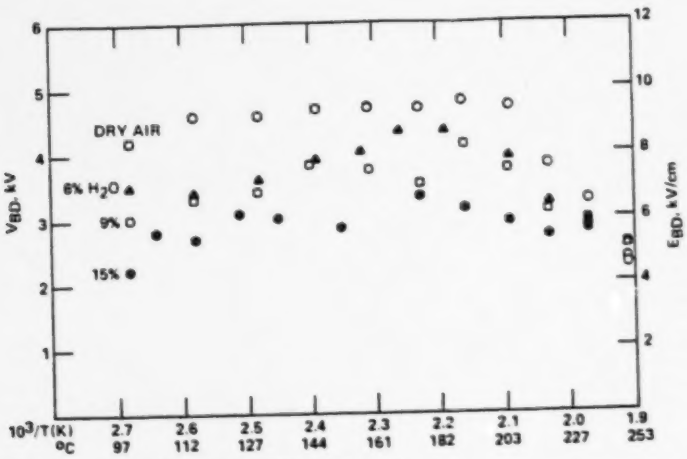

Figure 2. Electrical breakdown of Wabamun fly ash.

that, on average, an additional 2 kV/cm was necessary to produce a second microspark after the first breakdown signal was observed. As the field was further increased, the frequency of microsparks also increased until sparking began to occur at fields of about 11 to 12 kV/cm.

Several features of the breakdown behavior are evident in spite of the scatter in the data. First, the magnitude of V_{BD} for a given humidity level depends only weakly on the temperature, with the greatest variation occurring in the range of 180 to 250°C. This corresponds to the volume conduction region of the resistivity curve shown in Figure 3. In the region where surface conduction dominates (100 to 140°C), the magnitude of V_{BD} is relatively constant for a given water level. This is in marked contrast to the rapidly changing resistivity characteristic of the fly ash in the same region, as shown by Figure 3. Generally, increasing the water vapor in the test environment decreases V_{BD}. However, there is a much larger overall difference between the magnitudes of V_{BD} for the dry and moist ash layers than between samples at different levels of moisture in this surface conduction region. And in the high temperature (volume conduction) limit, all the data tend to converge.

The greatest variation of the magnitude of V_{BD} between the three dust species at identical test conditions occurs in dry air where differences of 1 to 1.5 kV are sometimes seen. In humid air, the magnitudes of V_{BD} for all dusts are quite similar, as illustrated in Figure 4 for 9 percent water vapor. This behavior is very different from that of the resistivity characteristics shown in Figure 5 for the same conditions. Here the resistivity varies by over two orders of magnitude between dust species.

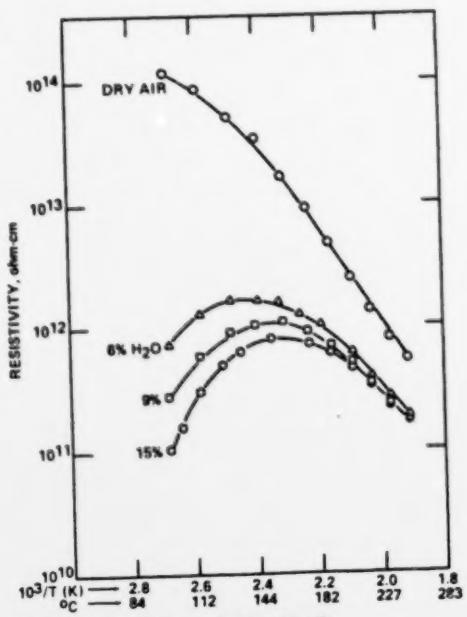

Figure 3. Resistivity of Wabamun fly ash.

Particle Size Effect on Breakdown

The influence of particle size on the breakdown behavior of Wabamun fly ash is shown in Figure 6 for 9 percent water vapor. The results are similar for other humidity levels. "Ordinary distribution" refers to the as-received ash while the two size-fractionated distributions are labeled according to their mass-median-diameter (MMD). Both the fine sample and the coarse sample for the two fly ashes had breakdown voltages higher than the ordinary distribution, with the coarse sample producing the largest increase. The corresponding resistivity characteristic for the Wabamun ash is shown in Figure 7. The coarse distribution is about an order of magnitude higher in resistivity than the ordinary distribution, but the fine and ordinary distributions are coincident.

Scanning electron microscope photographs of particles from the three distributions of fly ash showed that the ordinary distribution contained particles which were predominantly spherical and amorphous, with only a few relatively large, irregularly shaped particles. The fine fraction sample was nearly all spherical particles while the coarse fraction sample had an abundance of larger, irregularly shaped particles. The size-fractionated samples were analyzed by mercury porosimetry[4] to see how void dimensions differed between the distributions. The largest void radius detected by the porosimeter and the mean void radius calculated from the relative void population were determined for each sample and are shown in Table II.

The cement dust was composed of particles having no symmetry. The fine-fraction particles of this dust were relatively uniform in size with only a few larger particles. The resistivity characteristics were similar to those of the fly ashes. However, the fine-fraction breakdown behavior with moisture present was exceptionally erratic. The coarse-fraction exhibited consistently higher V_{BD} values than the other two distributions, as in the case of fly ash. But considering

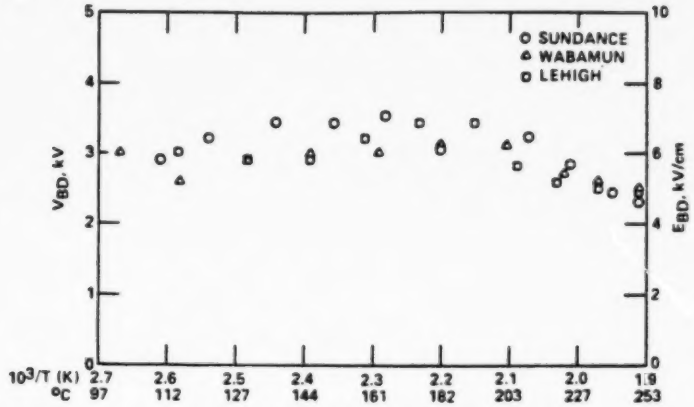

Figure 4. Electrical breakdown of all dust species for 9 percent water vapor.

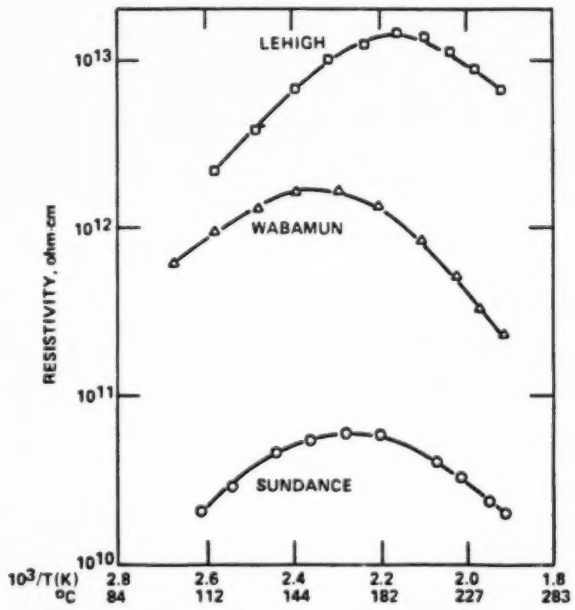

Figure 5. Resistivity of all dust species for 9 percent water vapor.

the scatter in individual data sets, the ordinary and fine-fraction data were virtually identical.

Compaction Effect on Breakdown

The effect of compaction on the breakdown behavior of the ordinary distributions of the three dusts was studied by increasing the surfce areal loading of the samples to about 2500 g/cm^2 in a laboratory press. In the case of fly ash, this had essentially no effect on the breakdown behavior. However, a slight effect was noted in the breakdown of the Lehigh cement dust (Figure 8). Here the increased compression of the dust layer resulted in a lowering of V_{BD} with a concomitant decrease in resistivity (Figure 9).

Discussion

The electron avalanche breakdown of a gas-filled gap is conventionally interpreted using Paschen's Law, which states that the breakdown potential across the gap is a function of the product of pressure and gap height. Typical data obtained by Earhart[5] for an air gap at different temperatures are shown in Figure 10. In general, the minimum in the curve broadens and shifts to the right as the temperature of the gap is increased, accompanied by a decrease in the slope of the linear portion to the right of the minimum. By assuming the laboratory pressure to be 1 atmosphere, the gap

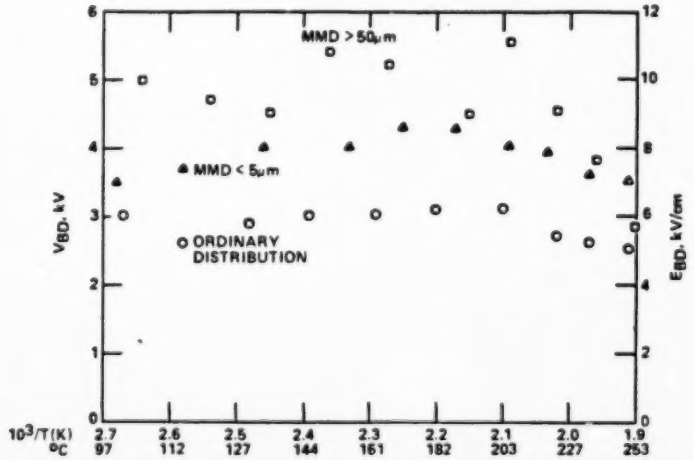

Figure 8. Electrical breakdown of size-fractionated Wabamun fly ash.

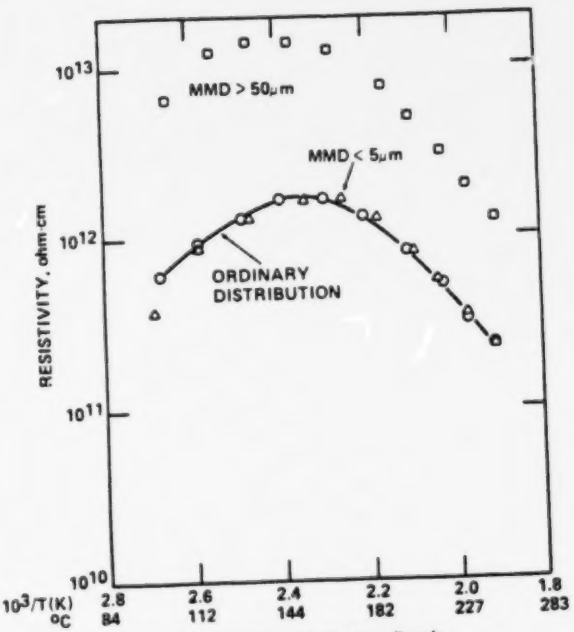

Figure 7. Resistivity of size-fractionated Wabamun fly ash.

distance corresponding to the minimum can be calculated for the three temperatures. This results in values of about 11, 14, and 17 μm for 22, 155, and 260°C, respectively. Mercury porosimetry analysis of the samples showed voids ranging from about 1.8 nm to several tens of micrometers in radius. The radius of the largest interparticle void for each sample is shown in Table II. Thus, voids of the size derived from Figure 10 do exist within these samples.

The product of pressure and gap height is essentially a measure of the number of molecules an electron will encounter while traversing the gap in the direction of the field. But the number of molecules in the gap will depend on gas density, rather than on pressure alone. Thus, a more general expression of Paschen's Law would use the product of gas density and gap height to describe the breakdown potential. Indeed, Earhart found that, for a given gap distance, a single curve (with the same qualitative features as those in Figure 10) was obtained when data for the breakdown potential at various temperatures was plotted as a function of gas density. Then for densities greater than that corresponding to the minimum in the Paschen curve, the potential necessary to cause breakdown increases in a linear fashion. Alternatively, if the density decreases below the value at the minimum, the breakdown potential would increase very rapidly. The temperature range used in the present experiments corresponds to only about a 30 percent change in the gas density. The slow variation of the breakdown potential with temperature suggests that breakdown was occurring in the region to the right of the minimum in the Paschen curve.

Assuming an average breakdown voltage of 400 volts from Figure 10 and dividing this by the calculated gap distances at the Paschen minimum, gives field strengths in the range of 235 to 365 kV/cm. However, average field strengths within the dust layer at breakdown in this study were 4 to 10 kV/cm. An enhanced local electric field in a void, E_{loc}, must then correspond to the breakdown field of Paschen's law. The average field and locally enhanced field should be related so that Paschen's Law can also be applied to V_{BD}. In part II of this work, it will be shown how such enhancements of the local electric field are obtained.

The general trend of decreasing V_{BD} with increasing levels of humidity is opposite to the behavior of an air-filled gap between two electrodes where it is observed that breakdown potential increases with increasing water vapor. In this latter case, the increase is attributed to an electron attachment and conversion process which occurs when water vapor is present.[6] However, the data for the present work indicate that the primary interaction of water vapor is with the surface of the dust layer particles (and consequently with the conduction mechanism prior to breakdown) rather than with the gas molecules in the void. This is in agreement with studies showing the dramatic effect of the presence of water vapor on surface resistivity.[2]

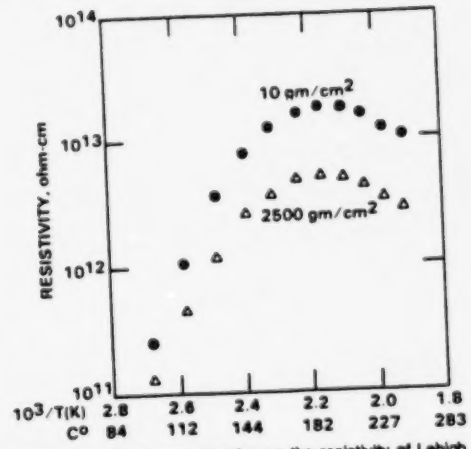

Figure 9. Effect of compaction on the resistivity of Lehigh cement dust.

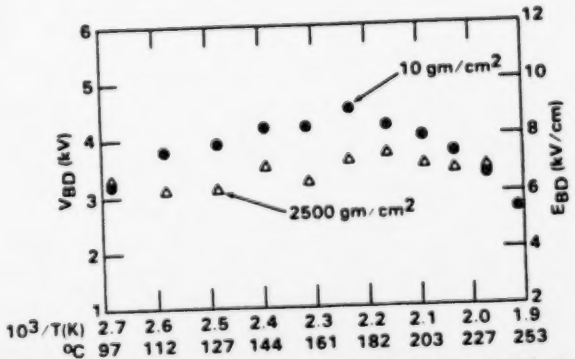

Figure 8. Effect of compaction on the electrical breakdown of Lehigh cement dust.

Paschen's Law aids in interpreting the effect of the particle size on V_{BD}. Assuming a void of the correct dimension exists in the dust layer, the first microspark will occur at a potential corresponding to the minimun in the Paschen curve. But since breakdown is statistical in nature, the probability that breakdown will occur is equal to the product of the probability of finding a given void in the dust layer and the probability that the local electric field enhancement will be sufficient to initiate the breakdown. One parameter that can be used to characterize the distribution of void sizes (and thus, the probability of the existence of a given void dimension near the minimum in the Paschen curve) is the mean void size of the sample. The coarse-fraction sample of the two fly ashes consists of particles much larger (on the average) than those of the ordinary distribution, resulting in

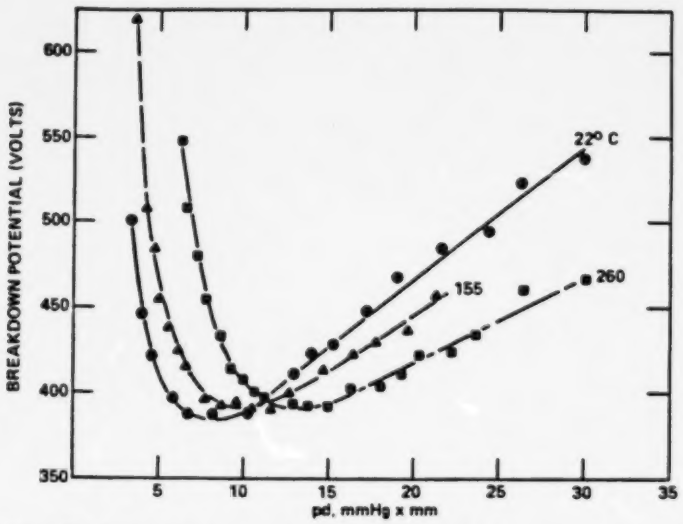

Figure 10. Paschen curves for breakdown in air from reference 5.

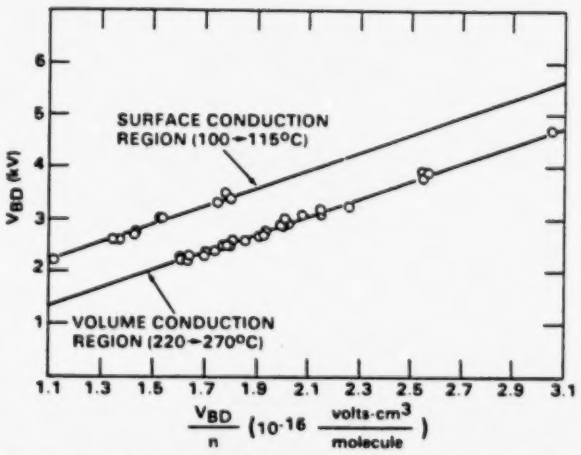

Figure 11. Plot of Equation 3 in the volume and surface conduction regions for all humidity levels of Wabamun fly ash.

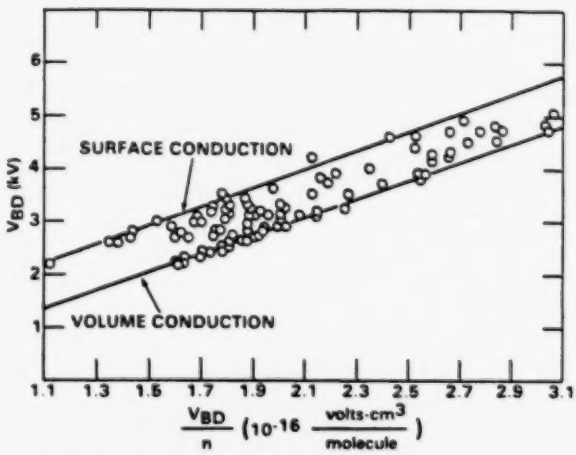

Figure 12. Plot of Equation 3 for all Wabamun fly ash data.

larger average void dimensions in the coarse sample. This is supported by the porosimetry data of Table II where the mean void radius, calculated on the basis of void distribution in the 4–200 μm range, for each distribution is shown. Paschen's Law then predicts a larger breakdown potential for this coarse sample than for the ordinary distribution. The case for the fine-fraction sample is similar when the porosity of this sample is considered. As shown in Table II, the ordinary distribution of Wabamun fly ash has a porosity of about 49 percent; while the fine distribution has a porosity of about 66 percent, due to agglomeration of the smaller particles. This suggests that the fine sample also contains larger voids than does the ordinary distribution. The porosimetry data for mean void radius in Table II support this conclusion. Thus, Paschen's Law predicts higher breakdown potentials. Moreover, porosimetry shows the average void dimension of the fine sample to be less than that of the coarse sample and is consistent with the data of Figure 6.

The mechanical compression used to change the surface areal loading of the fly ashes had no effect on their breakdown voltage. Apparently, the predominantly spherical particles of these dusts pack so efficiently that the mechanical loading could not further pack the samples and change their void dimensions. In the case of cement dust, the void dimension could be decreased by compressing the sample, and the breakdown voltage was lowered (Figure 8).

Having used Paschen's Law to explain the qualitative features of the breakdown data, we now proceed to show that the data do indeed obey Paschen's Law. One form of the expression for Paschen's Law is[7]:

$$V_{loc} = \frac{Cnd}{\ln\left(\frac{Dn}{\alpha}\right)} \qquad (1)$$

where V_{loc} is the local enhanced voltage across the void at breakdown; n, the gas density (molecules/cm^3); d, the void dimension; α, the Townsend primary ionization coefficient; and C and D, constants related to the gas. For these data, d represents the critical dimension of a void in the dust layer where breakdown first occurs.[8]

It is assumed that d and α change slowly enough with variations in the gas density over a limited temperature

range that they can be considered constants in this analysis. Furthermore, the logarithm can be expanded, retaining only the linear term, as

$$\ln\left(\frac{Dn}{\alpha}\right) = \frac{Dn}{\alpha} - 1, \tag{2}$$

since it is found that $0.8 < Dn/\alpha < 1.1$. Thus, Paschen's Law can be reduced to a straight line approximation:

$$V_{loc} \simeq m\left(\frac{V_{loc}}{n}\right) + b, \tag{3}$$

where

$$m = \frac{\alpha}{D} \text{ and } b = \frac{C\alpha d}{D}.$$

If the average applied voltage at breakdown is proportionally related to V_{loc} then the form of Equation 3 can be applied to V_{BD} as well.

Because α is a function of temperature, it is necessary to restrict the use of Equation 3 to a narrow temperature range. Figure 11 shows the result of plotting Equation 3 for V_{BD} using the breakdown data of Wabamun fly ash for all moisture levels in the two temperature limits shown. A straight line for each temperature limit results, indicating that these data obey Paschen's Law. Moreover, the slope of these lines results in values of (Dn/α) between 0.8 and 1.1 as n varies. Figure 12 shows the same two lines with all available data. The data corresponding to temperatures where both the volume and surface conduction mechanisms are important fall between the two lines.

Conclusions

The results of this work lead to the following conclusions concerning the onset of electrical breakdown in dust layers:

1. Electrical breakdown is an ordinary electron avalanche process originating in voids within the dust layer and obeying Paschen's Law. The size of voids where breakdown occurs appears to be in the range of 10 to 20 μm for the layers used.
2. Both a fine and coarse distribution of fly ash had mean void dimensions greater than the as-received distribution and exhibited correspondingly higher breakdown voltages.
3. Moderate mechanical compression had no effect on fly ash but did decrease the mean void dimensions in cement dust, resulting in lower breakdown voltages.

Acknowledgment

This work has been sponsored by the Air and Energy Engineering Research Laboratory of EPA (Cooperative Agreements CR-808973 and CR-810284).

References

1. R. E. Bickelhaupt, "Electrical volume conduction in fly ash," *J APCA* 24: 251 (1974).
2. R. E. Bickelhaupt, "Surface resistivity and the chemical composition of fly ash," *J APCA* 25: 148 (1975).
3. P. P. Budenstein, "On the mechanism of dielectric breakdown of solids," *IEEE Trans. Electr. Insul.* 15: 225 (1980).
4. S. Lowell, J. E. Shields, *Powder Surface Area and Porosity*, 2nd Ed., Chapman and Hall, New York, 1984, pp. 87–120.
5. R. F. Earhart, "The discharge of electricity through gases at various temperatures," *Phys. Rev.* 31: 652 (1910).
6. H. F. A. Verhaart, P. C. T. van der Laan, "The influence of water vapor on avalanches in air," *J. Appl. Phys.* 55: 3286 (1984).
7. E. Husain, R. S. Nema, "Analysis of Paschen curves for air, N_2 and SF_6 using the Townsend breakdown equation," *IEEE Trans. Electr. Insul.* 17: 350 (1982).
8. R. B. Mosley, P. R. Cavanaugh, J. R. McDonald, L. E. Sparks, "Measurements of Electrical Properties of Fly Ash Layers," U.S. EPA Third Symposium on the Transfer and Utilization of Particulate Control Technology: Volume II, EPA-600/9-82-005b, July 1982.

Dr. Young is a research physicist and Dr. DuBard is head of the Applied Technology Division of the Environmental Sciences Department at Southern Research Institute, P.O. Box 55305, Birmingham, AL 35255-5305. Dr. Sparks is a project officer at the U.S. Environmental Protection Agency, Air and Energy Engineering Research Laboratory, Research Triangle Park, NC 27711.

This paper was submitted for peer review May 2, 1986; the revised manuscript was received October 5, 1987.

ORD CLEARANCE FORM

1. EPA Report No.	2. Series	3. Lab/Office Draft No.	4. Copyright Permission
600/J-88/253	J	AEERL-P-344/-345	☐ Yes (Attached) ☒ No ☐ N/A

5A. Original Document Title:

The onset of electrical breakdown in dust layers: I. Microsparking described by Paschen's Law (-344); II. Effective dielectric constant and local field enhancement (-345)

5B. Final Document Title, if changed:

NA

6. Author(s), Affiliation, and Address (identify EPA authors with Lab/Office)

R. P. Young/J. L. DuBard (SoRI, P. O. Box 55305, Birmingham, AL 35255-5305); L. E. Sparks (EPA/AEERL)

7. Project Officer/FTS Telephone

Leslie E. Sparks/629-2458

8. Contract/IAG/Assistance Agreement No.

CR808973 and CR810284

9. Product (check one)

- ☒ Peer Reviewed Journal Article (complete block 13)
- ☐ Published Reports: Project Report/Summary (magnetic tapes/floppy diskettes), Method, Research Report, User's Guide, Design Manual, Handbook, Criteria Document, Health Assessment Document, Technology Transfer Report, Proceedings (Conferences, Symposia, Workshops)
- ☐ Symposium Papers and Book Chapters
- ☐ Internal Report (distribution restricted to EPA)
- ☐ Miscellaneous (newsletter, research brief, trade paper) non-peer reviewed journal article (complete block 13)
- ☐ Unpublished Report

10. DU/Obj./PPA/Project/Deliverable Output No.

DU = A119

11. Technical Information (Program) Manager

Signature W. W. Whelan, MD-64 — Date 11/17/87

Signature of sender (if other than TI(P)M) — Date to CERI

12. Signature/Date

L. E. Sparks, MD-54 — 11/4/87

W. G. Tucker, MD-54 — 11/5/87

E. L. Plyler, MD-54 — 11/6/87

11/6/87

13. Bibliographic Citation (Include Month/Year)

☒ Accepted 10/87 ☐ Published 11/88 (-344)

APCA J., Vol. 38, No. 11, pp. 1412-18 (-344).

14. Distribution (use block 16, if necessary)

15A. This Publication

- ☒ does not have policy implications for EPA
- ☐ has policy implications for EPA (memo attached)

15B. Lab/Office Director Signature

F. T. Princiotta, MD-60 Dir:AEERL

15C. Date

11/6/87

16. Comments

APCA J. is refereed; local peer review not required.

EPA-362(Cin)(Rev.3/87)